Rydberg Polaritons in a Cavity: A Superradiant Solid

Xue-Feng Zhang (张学锋),[1] Qing Sun (孙青),[2] Yu-Chuan Wen (文渝川),[3] Wu-Ming Liu,[2] Sebastian Eggert,[1] and An-Chun Ji (纪安春)[3,*]

[1]*Physics Department and Research Center OPTIMAS, University of Kaiserslautern, 67663 Kaiserslautern, Germany*
[2]*Institute of Physics, Chinese Academy of Sciences, Beijing 100190, China*
[3]*Department of Physics, Capital Normal University, Beijing 100048, China*

(Received 6 December 2012; published 26 February 2013)

We study an optical cavity coupled to a lattice of Rydberg atoms, which can be represented by a generalized Dicke model. We show that the competition between the atom-atom interaction and atom-light coupling induces a rich phase diagram. A novel superradiant solid (SRS) phase is found, where both the superradiance and crystalline orders coexist. Different from the normal second order superradiance transition, here both the solid-1/2 and SRS to SR phase transitions are first order. These results are confirmed by large scale quantum Monte Carlo simulations.

DOI: 10.1103/PhysRevLett.110.090402 PACS numbers: 05.30.Jp, 03.75.Nt, 42.50.Pq, 67.10.Fj

The study of quantum many-body problems and quantum phase transitions (QPT) has attracted great interest, and is currently one of the main issues in the condensed matter community [1]. In the past decade, the successful control of the interaction strength and dimensionality of ultracold quantum gases has made it possible to explore many interesting physical phenomena [2]. For example, the observation of the superfluid-Mott insulator transition [3], a Tonks gas [4], the BEC to BCS crossover [5], and the Kosterlitz-Thouless phase transition [6] have all been established in ultracold quantum gases.

More recently, ultracold atoms have been combined with cavity QED [7,8] to study atom-light coupled many-body problems, which give rise to new phenomena. In particular, when the two-level atom gas is coupled to a cavity [9], the coherent nonlocal atom-light interaction supports the famous superradiance (SR) phase transition in the Dicke model (DM) [10,11]. This SR phase is formed by the condensation of atom-light coupled polaritons [12] and breaks the U(1) symmetry. However, the interactions between atoms, which may bring new phenomena or induce novel QPTs, are not considered in the DM.

Atom-atom interactions promise to give interesting new effects and can be implemented via Rydberg atoms [13–19]. The unique properties of strong dipole-dipole interactions and quite long lifetimes have made them a powerful tool for the implementation of coherent blockade effects and quantum information [13]. Especially, the successful trapping of Rydberg atoms in a 1D optical lattice [14,15] has stimulated the study of many-body quantum systems, such as spin systems [16,17] and dynamical crystallization or melting of ultracold atoms [18–20].

In this Letter, we consider a 1D lattice of Rydberg atoms coupled to an optical cavity, where the dipole interaction competes with the atom-light coupling. Such a system can be described by a generalized DM. We see that, while the atom-light interaction favors the SR phase, the atom-atom interaction tends to form three incompressible Rydberg solid states with filling numbers 0, 1/2, and 1, which destroy the coherence of the cavity field. Most importantly, we find a novel state corresponding to a "superradiant solid" (SRS) phase, where both the superradiance and crystalline orders coexist and the corresponding U(1) and translation symmetries are broken simultaneously. Compared with the supersolid (SS) phase in an optical lattice [21–23], which breaks the same symmetries, the SRS is rather unique as it is induced by the nonlocal atom-light coupling and the condensation of polaritons. Moreover, we find that while the solid-(0, 1) to SR phase transitions remain second order, both the solid-1/2 and SRS to SR phase transitions become first order.

The system under investigation is schematically depicted in Fig. 1(a), where we have considered an

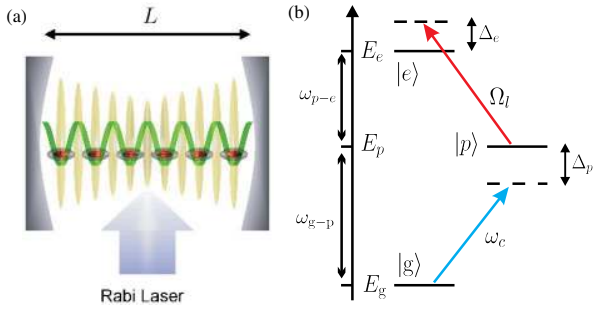

FIG. 1 (color online). (a) Schematic diagram of a 1D lattice of atoms trapped inside an ultrahigh finesse optical cavity. Each site is tuned to locate at the antinode of the cavity mode and occupied by a single atom with the ground state $|g\rangle$ coupled to a high-lying Rydberg state $|e\rangle$ via a two-photon transition process. (b) Setup for the internal energy levels of the atoms, where the cavity mode transits the ground state $|g\rangle$ to an intermediate state $|p\rangle$ with a large detuning $\Delta_p = \omega_c - \omega_{g-p}$ (ω_{g-p} is the transition frequency between $|g\rangle$ and $|p\rangle$ states), while the transition $|p\rangle \rightarrow |e\rangle$ of frequency ω_{p-e} is driven by a laser with Rabi frequency Ω_l and frequency ω_l detuned by $\Delta_e = \omega_l - \omega_{p-e}$.

ultrahigh-finesse optical cavity with λ_c the cavity wavelength and g_0 the single-atom coupling rate. We add an optical lattice with N sites into the cavity along the cavity axis. Each site is occupied by a single atom with the ground state $|g\rangle$ coupled to a high-lying Rydberg state $|e\rangle$ via a two-photon transition process [24] [Fig. 1(b)], where the cavity mode transits the ground state $|g\rangle$ to an intermediate state $|p\rangle$ with a large detuning Δ_p, and $|p\rangle$ is coupled to $|e\rangle$ by a laser with Rabi frequency Ω_l and frequency ω_l detuned by Δ_e. When Δ_p is large, the intermediate state $|p\rangle$ can be eliminated adiabatically and we arrive at the effective Hamiltonian of site i with $H_i^{\text{eff}} = -\Delta|e_i\rangle\langle e_i| + g(\psi|e_i\rangle\langle g_i| + \text{H.c.})$ in the rotating-wave approximation, where $g = g_0^*\Omega_l/|\Delta_p|$ is the effective coupling constant, $\Delta = \Delta_p + \Delta_e$ is the total detuning and $\psi^\dagger$ is the single-mode creation operator of the cavity field. Then, by performing a unitary transformation to the new rotating frame (see the Supplemental Material [25] for details), and extend the above two-photon transition process to a 1D lattice of atoms coupled to the cavity field, we derive the following effective Hamiltonian of the system [26]

$$H = \omega_c\psi^\dagger\psi + \sum_{i=1}^{N}\frac{\epsilon}{2}(b_i^\dagger b_i - a_i^\dagger a_i) + g\sum_{i=1}^{N}(b_i^\dagger a_i\psi + \text{H.c.}) + V\sum_{\langle i,j\rangle}P^{(i)}P^{(j)} - \mu N_{\text{ex}}, \quad (1)$$

where $\epsilon = \omega_c - \Delta$ is the effective transition frequency. Here we have introduced the boson operators a_i and b_i to represent the lower level $|g_i\rangle$ and upper level $|e_i\rangle$ of each atom i with the single-occupancy constraint $b_i^\dagger b_i + a_i^\dagger a_i = 1$. We consider a uniform atom-light coupling, which can be realized conveniently by tuning the optical lattice spacing a [14] to match the cavity wavelength. In view of normalization of photons, here we rescale $g \equiv \bar{g}/\sqrt{N}$ as usual. The strong dipole interactions between two Rydberg states is modeled by projectors $P^{(i)} = (1+\sigma_z^{(i)})/2$ onto the Rydberg state with $\sigma_z^{(i)} \equiv b_i^\dagger b_i - a_i^\dagger a_i$, where only nearest neighbor (NN) interactions with $V = C_6/a^6$ are considered [16]. The last term is the chemical potential for the total number of excitations $N_{\text{ex}} = \psi^\dagger\psi + \sum_{i=1}^{N} b_i^\dagger b_i$ in the grand canonical ensemble.

We start by discussing two limiting cases possessed in the above model. First, for $V = 0$ the Hamiltonian (1) becomes the DM. Here we note that, because the ground state $|g\rangle$ of the atoms is not directly coupled to the Rydberg state $|e\rangle$, the so called no-go theorem [27] does not apply [28], and the SR phase can occur. Recently, the SR phase transition has been observed with a superfluid atomic gas in an optical cavity [9]. Second, when g is zero this system becomes a pure lattice of Rydberg atoms. Then by tuning the chemical potential $\tilde{\mu} \equiv \mu - \omega_c$, one may derive three "incompressible" Rydberg solid states [29]: (i) $\tilde{\mu} < -\Delta$, it forms a solid-0 phase with all the atoms staying in the ground state; (ii) $-\Delta < \tilde{\mu} < 2V - \Delta$, half of the atoms are excited to the Rydberg states and form a solid-1/2 phase with staggered order because of the nearest neighbor repulsion; (iii) $\tilde{\mu} > 2V - \Delta$, all the atoms are excited to the Rydberg states forming a solid-1 phase.

In the region between two such limits, the competition of the atom-cavity interaction and the Rydberg atom-atom repulsion may induce an intermediate phase. This invites the question if it is possible to condense the atom-light coupled polaritons to break the U(1) symmetry and at the same time also break the translational symmetry, which would be called a superradiant solid (SRS). In general, it is quite rare to find systems which show long range phase coherence and at the same time have spontaneously broken translational invariance. In this respect the SRS phase is reminiscent of the supersolid (SS) phase in the 1D Bose-Hubbard model for the soft-core contact interaction [23]. However, the SRS phase here arises from the *nonlocal* atom-cavity coupled system. The Rydberg atom-atom interaction extends naturally over a longer range causing the previously unknown state of matter beyond the traditional Dicke model. In contrast to the previously studied SS phase for bosons in other lattice systems, the SRS phase is formed by the coherent cavity field combined with the inherent coherence of the two-level atoms and possesses a crystalline order at the same time. Furthermore, this does not require frustration or soft-core interactions nor an artificial longer range particle interactions. In this Letter, we use an analytical variational approach and numerical QMC simulation to study a possible SRS phase in detail.

We introduce a variational ground wave function [12] which can describe crystalline order and a superradiant phase simultaneously

$$|\lambda,\theta\rangle = \exp\left(\frac{\lambda\sqrt{N}\psi^\dagger}{2}\right)\prod_i\left[\cos\left(\frac{\theta_i}{2}\right)b_i^\dagger + \sin\left(\frac{\theta_i}{2}\right)a_i^\dagger\right]|0\rangle, \quad (2)$$

where $|0\rangle$ denotes the vacuum state with all atoms in the ground state, and λ and θ_i are the variational parameters for the coherent cavity field and atomic fields. To find the ground state, we calculate the energy density $\mathcal{E} \equiv 4\langle\lambda,\theta|H|\lambda,\theta\rangle/N$:

$$\mathcal{E} = 4[-\bar{g}\lambda(\sin\theta_C + \sin\theta_D) + V\cos\theta_C\cos\theta_D - \tilde{\mu}\lambda^2 - (\tilde{\mu} + \Delta - V)(\cos\theta_C + \cos\theta_D)], \quad (3)$$

where we have assumed two sublattices C and D which allows us to describe the most dominant possible order of the solid-1/2. From Eq. (3) we see that while the $\bar{g}$ term tends to enhance the cavity field λ and the condensation of polaritons, the second V term favors the staggered order of the polaritons. After minimizing $\mathcal{E}$ in respect to the variational parameters, we derive the phase diagram Fig. 2. The corresponding variational values are shown in Table I, where the solid phases represent the Rydberg crystals

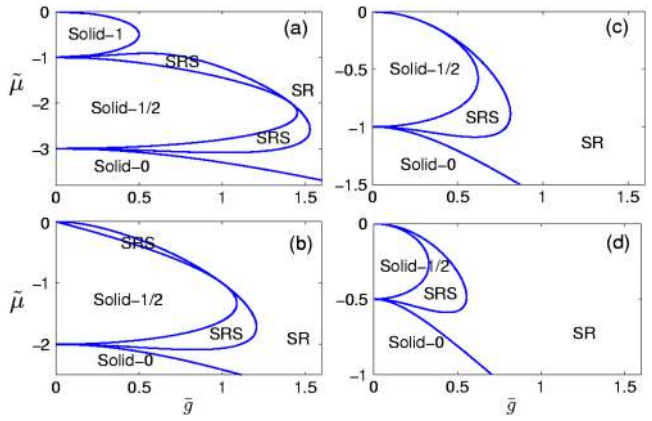

FIG. 2 (color online). Variational phase diagram for (a) $\Delta = 3$, (b) $\Delta = 2$, (c) $\Delta = 1$, and (d) $\Delta = 0.5$. All the parameters are in units of V.

without coherent cavity excitations. The usual superradiance phase is denoted by SR, where the atoms and light form polaritons and condense with a nonzero order parameter $\langle b_i^\dagger a_i \rangle = \sin\theta_{\mathrm{SR}}/2$ and a coherent cavity field λ_{SR}. The most interesting finding is that, when $\bar{g} \sim V$ there exists an intermediate SRS phase between the solid-1/2 and SR phases. Different from the SR phase where the polaritons are excited uniformly, the SRS phase also breaks the translation symmetry, which shows a characteristic excitation density $\rho_{C,D} = (\cos\theta_{1,2} + 1)/2$ that is not equal on the two sublattices. Therefore, both the superradiance and crystalline orders coexist in the SRS phase. In Fig. 2, we also see that the solid lobes shrink with decreasing Δ.

However, the above results are derived from mean-field calculations, so the SRS phase may not be stable when quantum effects are taken into account. In particular, when an additional Rydberg excitation is introduced (as a quasiparticle) into or removed (as a quasihole) from the solid-1/2 phase, the strong quantum fluctuation of the nonlocal atom-cavity coupling may drive the particle (or hole) to move freely on the whole lattice, which may destroy the staggered solid order and drive the solid-1/2 phase directly into the SR phase. Another possibility is that the SRS phase may be unstable and separates into domains [22]. To settle these issues and demonstrate explicitly the phase diagram, an unbiased numerical simulation is necessary.

We adopt the high-accuracy Stochastic Cluster Series Expansion (SCSE) algorithm [30,31] (see the Supplemental Material [25] for details), which is very efficient for simulating the system with long range interactions. In order to distinguish different phases, one needs to calculate several observables—the average excitation density $\rho = \langle N_{\mathrm{ex}} \rangle / N$, the structure factor $S(q)/N = \langle |\sum_{k=1}^{N} n_k e^{\mathbf{i} q r_k}|^2 \rangle / N^2$, and the compressibility $\kappa_T = N\beta(\langle \rho^2 \rangle - \langle \rho \rangle^2)$. For the half filled solid-1/2 phase, we take the structure factor $S(Q)/N$ with staggered order $Q = \pi$ to characterize the translational symmetry breaking.

Figure 3(a) shows the zero-temperature phase diagram for $\Delta = 3$ and $V = 1$. Compared with the mean-field results the SRS phase is greatly suppressed, indicating that quantum fluctuations weaken the SRS order. Nonetheless, the SRS phase remains stable in a small region as shown in the enlarged region of the SRS phase in Fig. 3(c). At first sight it appears difficult to reach such narrow regions of the SRS phase experimentally. However, this changes when considering the ρ-$\bar{g}$ phase diagram in Fig. 3(b), where the SRS phase exists in a wide region $\Delta\rho \approx 0.1$ in the excitation density. In Fig. 3(b) we also find that the region of the particle-excited SRS phase is smaller than the hole-excited one. The phase separated (PS) regions show that both the solid-1/2 and the SRS to SR phase transitions are first order. This differs from the mean-field results and may be understood by the Ginzburg Landau theory [32]: Because the U(1) and translation symmetries are broken simultaneously, the corresponding order parameters $S(Q)/N$ and $\langle b_i^\dagger a_i \rangle$ couple to each other and contribute to a sixth-order term in the free energy, which results in the first order phase transition. Moreover, a tricritical point appears among the SRS, SR, and solid-1/2 phases, see Fig. 3(c).

To provide a convincing support for the above phase diagram, we now concentrate on the properties of the phase

TABLE I. The variational values for different phases, where $\theta_1 \neq \theta_2$ in the SRS phase. These values are determined by minimizing Eq. (3) which give rise to the phase diagram of Fig. 2.

Variational values	Solid-0	SRS	SR	Solid-1/2	Solid-1
θ_C	π	θ_1	θ_{SR}	0	0
θ_D	π	θ_2	θ_{SR}	π	0
λ	0	λ_{SRS}	λ_{SR}	0	0

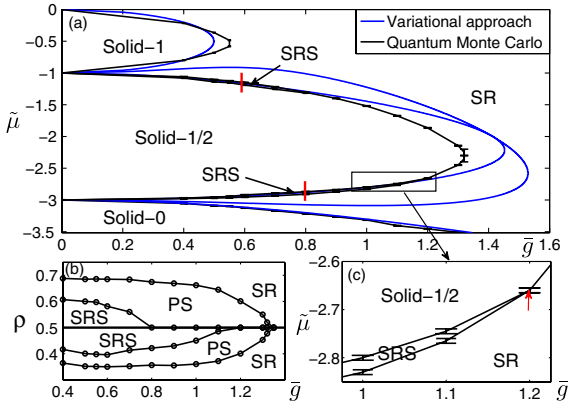

FIG. 3 (color online). (a) The μ-$\bar{g}$ phase diagram obtained by different methods for $V = 1$ and $\Delta = 3$ in the grand-canonical ensemble. The red solid vertical lines are the traces evaluated in Fig. 4. (b) The ρ-$\bar{g}$ phase diagram obtained by QMC simulation. Here, PS denotes the phase separation between the solid-1/2, SRS, and SR phase transitions, see the context for detail. (c) The enlarged region of the SRS phase, where the red arrow marks the tricritical point among the SRS, SR, and solid-1/2 phases.

transitions. Figure 4 shows $S(Q)/N$ and $\kappa_T/10$ along the trajectories which are indicated by solid vertical lines (red) in Fig. 3(a). Here, we take $T = V/500$ which is low enough to avoid the thermal effect, and the typical lattice length $N = 100$. In both panels, there exist regions where a vanishing structure factor $S(Q)/N \to 0$ is accompanied by a finite κ_T, which means that the translational symmetry is not broken and they are compressible, which is characteristic of the SR phases. Regions of zero κ_T with finite $S(Q)/N$ correspond to the incompressible solid-1/2 phases. Most significantly, there exist intermediate SRS phases which have both finite $S(Q)/N$ and κ_T. The corresponding structure factor $S(Q)/N$ and average density excitation ρ have a finite jump and κ_T diverges on the critical points $\tilde{\mu} = \tilde{\mu}_c$. It indicates that the SR to SRS phase transition is first order. In Fig. 4, we also show the results for different Δ. We find that, while the region of the SRS phase in the left panel is hardly affected by Δ, the one in the right panel shrinks faster by decreasing Δ. This can be understood by the second-order atom-light interaction process which differs for a particle or hole excited state with corresponding second-order energies $E_p^{(2)} \sim -\frac{\bar{g}^2}{(\Delta - 2C_6)}$ and $E_h^{(2)} \sim -\frac{\bar{g}^2}{\Delta}$, respectively. Note that $|E_p^{(2)}| > |E_h^{(2)}|$, which means the particle excited SRS phase is harder to form than the hole excited one and more easily suppressed by decreasing Δ. After that, we also performed a scaling analysis for the system. We find that both $S(Q)/N$ and κ_T in the SRS phase converge to finite values with $N \to \infty$ (see the Supplemental Material [25]), which demonstrate that the existence of the SRS phase is robust in the thermodynamic limit.

Now, we discuss how to realize and identify the predicted new phases in experiments. We consider for

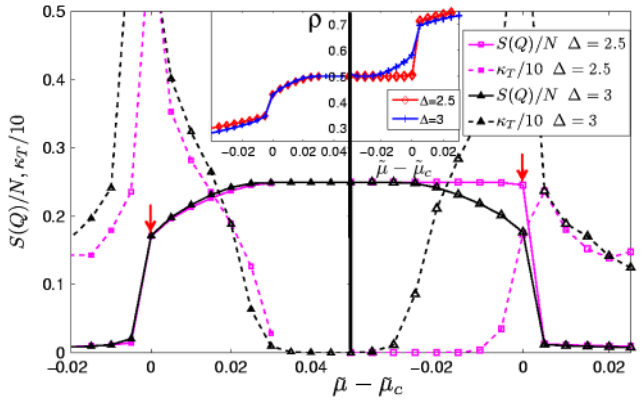

FIG. 4 (color online). The structure factor $S(Q)/N$ (solid line) and compressibility $\kappa_T/10$ (dashed line) along the trajectories of the lower (left panel) and upper (right panel) vertical cuts indicated by solid bars in Fig. 3(a). Here, the red arrows mark the critical points with $\tilde{\mu} = \tilde{\mu}_c$. For all cases $V = 1$, $\beta = 500$, $N = 100$, and $\Delta = 3$ ($\Delta = 2.5$). The inset shows the corresponding average excitation density ρ. For simplicity, the small error bars for the observables are not shown here.

illustration the experimentally achievable parameters: $\lambda_c = 850\,\text{nm}$, $L = 170\ \mu\text{m}$, $g_0/2\pi \approx 14.4$ MHz, $\kappa/2\pi \approx 0.66$ MHz [33] and a 1D lattice of ^{87}Rb atoms with the lattice spacing $a = 2\lambda_c$ and $N = 100$ sites are coupled to the cavity. The $5S_{1/2}$ ground state of ^{87}Rb atom is coupled to the $5P_{3/2}$ intermediate state with the detuning $\Delta_p/2\pi \approx 400$ MHz and the Rabi laser frequency Ω_l can be tuned continuously between $2\pi \times (0, 60)$ MHz, which give rise to the effective strength $\bar{g}/2\pi \approx (0, 21.6)$ MHz. Here, we have taken, for example, the principal quantum number of the $nS_{1/2}$ excited state $n = 34$, where only nearest neighbors interact significantly and the van der Waals coefficient $C_6/2\pi \approx 195\ \text{MHz}\,\mu\text{m}^6$ [34] with the NN interactions $V/2\pi \approx 11.3$ MHz. Under these parameters and with the total detuning $\Delta/V = 3$, we see that $\bar{g}/V$ varies between $(0, 1.91)$ and the wide regime of the phase diagram of Fig. 3 can be reached experimentally.

We then characterize the formation of the coherent phases, which should be observed on the time scale of the cavity damping. One may first pump the cavity field with the photon density $\rho = 0.45$ and then turn on the Rabi laser to set $\bar{g}/V \approx 1.4$. The system will be in the SR phase and the typical time of this coherent process is determined by the energy scale of the atom-cavity coupling $\bar{g}$, which is much larger compared to both decay rates of the cavity κ and of the Rydberg state with $\gamma \simeq 2\pi \times 1$ kHz. Then, by tuning $\bar{g}/V \approx 1.0$, the system may undergo a phase transition from SR to SRS phase. Both the two phases are characterized by the coherent cavity field and distinct polariton excitations which may be discriminated by the absorption imaging [35] or the usual Bragg spectroscopy methods. As for the 1/2-solid to SR phase transition, one may initially pump the 1D lattice of atoms into an 1/2-filling Rydberg crystal by two external Rabi lasers (see Ref. [14]) and then turn on $\bar{g}$. If $\bar{g}/V < 1.3$ there there will be no coherent light, and the system stays in the 1/2-solid phase. While for $\bar{g}/V > 1.3$ the system will be in the SR phase, and one may detect the leak of coherent cavity field in the time scale κ^{-1}.

In summary, we have shown that the generalized Dicke model of a cavity QED coupled with a Rydberg lattice gas displays a rich phase diagram. The competition between the nonlocal atom-light coupling and the atom-atom interaction can stabilize a novel SRS phase. By implementing an unbiased QMC calculation, we find that both the solid-1/2 and SRS to SR phase transitions are first order, and the hole-excited SRS phase is more stable than the particle-excited one. This system may act as a new quantum simulator for the future study of quantum many-body physics.

We acknowledge T. Wang for helpful discussions. This work is supported by NCET, NSFC under Grants No. 11704175 and No. 10904096, NSFB under Grant No. 1092009, NKBRSFC under Grant No. 2011CB921502, and by the DFG via the SFB/Transregio 49.

*andrewjee@sina.com

[1] S. Sachdev, *Quantum Phase Transitions* (Cambridge University Press, Cambridge, England, 1999).

[2] I. Bloch, J. Dalibard, and W. Zwerger, Rev. Mod. Phys. **80**, 885 (2008); I. Bloch, J. Dalibard, and S. Nascimbéne, Nat. Phys. **8**, 267 (2012).

[3] M. Greiner, M. O. Mandel, T. Esslinger, T. Hänsch, and I. Bloch, Nature (London) **415**, 39 (2002).

[4] B. Paredes, A. Widera, V. Murg, O. Mandel, S. Fölling, I. Cirac, G. V. Shlyapnikov, T. W. Hänsch, and I. Bloch, Nature (London) **429**, 277 (2004); T. Kinoshita, T. Wenger, and D. S. Weiss, Science **305**, 1125 (2004).

[5] Q. J. Chen, J. Stajic, S. N. Tan, and K. Levin, Phys. Rep. **412**, 1 (2005).

[6] Z. Hadzibabic, P. Krüer, M. Cheneau, B. Battelier, and J. Dalibard, Nature (London) **441**, 1118 (2006).

[7] F. Brennecke, T. Donner, S. Ritter, T. Bourde, M. Köhl, and T. Esslinger, Nature (London) **450**, 268 (2007).

[8] Y. Colombe, T. Steinmetz, G. Dubois, F. Linke, D. Hunger, and J. Reichel, Nature (London) **450**, 272 (2007).

[9] K. Baumann, C. Guerlin, F. Brennecke, and T. Esslinger, Nature (London) **464**, 1301 (2010).

[10] R. H. Dicke, Phys. Rev. **93**, 99 (1954).

[11] K. Hepp and E. H. Lieb, Ann. Phys. (N.Y.) **76**, 360 (1973).

[12] P. R. Eastham and P. B. Littlewood, Phys. Rev. B **64**, 235101 (2001).

[13] For a review, see M. Saffman, T. G. Walker, and K. Mølmer, Rev. Mod. Phys. **82**, 2313 (2010), and references therein.

[14] M. Viteau, M. G. Bason, J. Radogostowicz, N. Malossi, D. Ciampini, O. Morsch, and E. Arimondo, Phys. Rev. Lett. **107**, 060402 (2011).

[15] S. E. Anderson, K. C. Younge, and G. Raithel, Phys. Rev. Lett. **107**, 263001 (2011).

[16] B. Olmos, R. González-Férez, and I. Lesanovsky, Phys. Rev. Lett. **103**, 185302 (2009).

[17] I. Lesanovsky, Phys. Rev. Lett. **106**, 025301 (2011).

[18] T. Pohl, E. Demler, and M. D. Lukin, Phys. Rev. Lett. **104**, 043002 (2010).

[19] H. Weimer and H. P. Büchler, Phys. Rev. Lett. **105**, 230403 (2010).

[20] A. Lauer, D. Muth, and M. Fleischhauer, New J. Phys. **14**, 095009 (2012).

[21] P. Sengupta, L. P. Pryadko, F. Alet, M. Troyer, and G. Schmid, Phys. Rev. Lett. **94**, 207202 (2005).

[22] S. Wessel and M. Troyer, Phys. Rev. Lett. **95**, 127205 (2005).

[23] G. G. Batrouni, F. Hébert, and R. T. Scalettar, Phys. Rev. Lett. **97**, 087209 (2006).

[24] C. Guerlin, E. Brion, T. Esslinger, and K. Molmer, Phys. Rev. A **82**, 053832 (2010).

[25] See Supplemental Material at http://link.aps.org/supplemental/10.1103/PhysRevLett.110.090402 for the derivation of the two-photon transition, details of the quantum Monte Carlo simulations and the finite size scaling analysis.

[26] We should note that each atom of the 1D lattice can be excited independently here. This is in contrast to Ref. [24], where all the N atoms are in the blockade regime and excited collectively with only one Rydberg state.

[27] K. Rzążewski, K. Wódkiewicz, and W. Żakowicz, Phys. Rev. Lett. **35**, 432 (1975); I. Białynicki-Birula and K. Rzążnewski, Phys. Rev. A **19**, 301 (1979).

[28] J. Larson and M. Lewenstein, New J. Phys. **11**, 063027 (2009).

[29] Here we use ''incompressible'' to mean that an additional Rydberg excitation is forbidden by an infinitesimal change of chemical potential.

[30] For a general introduction of QMC, see D. P. Landau and K. Binder, *A Guide to Monte Carlo Simulations in Statistical Physics* (Cambridge University Press, Cambridge, England, 2005), Chap. 8.

[31] For more details on SCSE, we refer to A. W. Sandvik, Phys. Rev. B **59**, R14157 (1999); O. F. Syljuåsen and A. W. Sandvik, Phys. Rev. E **66**, 046701 (2002), and Supplemental Material [25].

[32] X. F. Zhang, R. Dillenschneider, Y. Yu, and S. Eggert, Phys. Rev. B **84**, 174515 (2011).

[33] K. W. Murch, K. L. Moore, S. Gupta, and D. M. Stamper-Kurn, Nat. Phys. **4**, 561 (2008).

[34] K. Singer, J. Stanojevic, M. Weidemüller, and R. Côté, J. Phys. B **38**, S295 (2005).

[35] K. D. Nelson, X. Li, and D. S. Weiss, Nat. Phys. **3**, 556 (2007).